DOI:10.1093/jnci/djs436



ARTICLE

# Toll-Like Receptor 3 Expressing Tumor Parenchyma and Infiltrating Natural Killer Cells in Hepatocellular Carcinoma Patients

Valerie Chew, Charlene Tow, Caleb Huang, Emilie Bard-Chapeau, Neal G. Copeland, Nancy A. Jenkins, Achim Weber, Kiat Hon Lim, Han Chong Toh, Mathias Heikenwalder, Irene Oi-Lin Ng, Alessandra Nardin, Jean-Pierre Abastado

Manuscript received June 6, 2012; revised August 2, 2012; accepted August 22, 2012.

**Correspondence to:** Jean-Pierre Abastado, PhD, Singapore Immunology Network (SIgN), Agency for Science, Technology and Research (A*STAR), 8A Biomedical Grove, Immunos, Biopolis, Singapore 138648, Singapore (email: abastado@immunol.a-star.edu.sg).

**Background** Hepatocellular carcinoma (HCC) is a highly aggressive cancer that is linked to chronically dysregulated liver inflammation. However, appropriate immune responses can control HCC progression. Here we investigated the role and underlying mechanism of toll-like receptor 3 (TLR3) in HCC.

**Methods** HCC cell death, and natural killer (NK) cell activation and cytotoxicity were assessed in vitro after treatment with the TLR3 ligand poly(I:C). The effect of TLR3 on the tumor parenchyma and infiltrating immune cells was investigated in a spontaneous liver tumor mouse model and a transplanted tumor mouse model (n = 3–9 mice per group). Immunohistochemistry and quantitative polymerase chain reaction were used to analyze tumor samples from 172 HCC patients. Paired *t*-tests and analysis of variance tests were used to calculate *P*-values. The relationship between TLR3 expression and survival was determined by the Kaplan–Meier univariate survival analysis and a log-rank test. All statistical tests were two-sided.

**Results** TLR3 activation increased cell death in the $TLR3^+$ SNU182 HCC cell line (30.5% vs 8.5%, $P = .03$) and promoted NK-cell activation (32.6% vs 19.4%, $P < .001$) and cytotoxicity (relative fourfold increase, $P = .03$) in vitro. In vivo, poly(I:C) treatment increased intratumoral chemokine expression, NK-cell activation and tumor infiltration, and proliferation of tumor-infiltrating T and NK cells. Proliferation of tumor parenchyma cells was decreased. Also, expression of chemokines or treatment with poly(I:C) decreased tumor growth. TLR3 expression in patient samples correlated with NK-cell activation, NK- and T-cell tumor infiltration, and inversely correlated with tumor parenchyma cell viability. TLR3 expression was also associated with longer survival in HCC patients (hazard ratio of survival = 2.1, 95% confidence interval = 1.3 to 3.4, $P = .002$).

**Conclusions** TLR3 is an important modulator of HCC progression and is a potential target for novel immunotherapy.

J Natl Cancer Inst 2012;104:1796–1807

Hepatocellular carcinoma (HCC) is the fifth most common cancer and the third leading cause of cancer-related death worldwide (1). Resection and transplantation are the most successful treatments for HCC; however, most patients relapse and overall survival remains poor. HCC is thought to result from persistent, nonspecific activation of the immune system within the chronically inflamed liver, causing repeated cycles of tissue damage, repair and regeneration, and eventually carcinogenesis (2,3). However, we have previously reported that expression of specific proinflammatory genes within the tumor microenvironment is associated with improved patient survival (4), suggesting a more complex role of the immune system in HCC.

Toll-like receptor 3 (TLR3) is one of the key proinflammatory genes associated with "good prognosis" in HCC (4). TLR3 is an endosomal receptor for double-stranded RNA and is expressed in several subsets of immune cells, including dendritic cells (5) and natural killer (NK) cells (6). TLR3 is also expressed by fibroblasts (7), lung epithelial cells (8), hepatocytes (9), and several types of tumor cells, including breast cancer and melanoma cells (10,11). TLR3 is involved in antiviral responses and the production of type I interferons (IFNs) (12). RNA from damaged tissues can also serve as a ligand for TLR3 (13,14). Synthetic TLR3 ligands, such as polyinosinic:polycytidylic acid [poly(I:C)] acts as potent immune adjuvants by enhancing dendritic cell cross-presentation and promoting $CD8^+$ T-cell responses (15,16). Such ligands have thus been used to treat a range of malignancies in a variety of clinical settings (17).

In vitro studies indicate that TLR3 activation triggers apoptosis of several tumor cell lines, including breast cancer (10) and melanoma (11). Moreover, transfection of TLR3 into HCC cell lines

renders them sensitive to poly(I:C)-induced killing (18). TLR3-expressing NK cells can also be directly activated by poly(I:C) (6,19). However, the role of TLR3 in HCC remains to be evaluated in human patients. We explored the role played by TLR3 in the apoptosis of HCC cells and assessed the contribution of this receptor to NK-cell activation and cytotoxicity using HCC cell lines, two in vivo mouse models, and patient samples and survival data.

## Materials and Methods

### Cell Lines and Reagents

The methods by which the HCC cell lines (Hepa1-6, SNU182, SNU368, SNU387, SNU-423, SNU449, SNU475, PLC/PR5, HuH-7, HepG2, Hep3B, and SK-HEP-1) were maintained are described in detail in the Supplementary Methods (available online). Endotoxin-free poly (I:C) and polyadenylic–polyuridylic acid [poly(A:U)] were obtained from InvivoGen (San Diego, CA). We assumed the authenticity of the cell lines was verified by the source.

All the antibodies used for immunohistochemistry, flow cytometry, or NK-cell depletion were listed in Supplementary Table 1 (available online). TLR3 was knocked down using predesigned stealth select RNAi (Invitrogen) according to the manufacturer's instructions (Supplementary Methods, available online).

### Patient Samples

Resected tumor samples were obtained from patients who underwent curative resection for HCC (n = 172) between 1991 and 2009 at the National Cancer Centre (Singapore), Queen Mary Hospital (Hong Kong, China), or the University Hospital of Zurich (Zurich, Switzerland). All samples were collected with written informed consent in compliance with the requirements of the local ethical committee at each institution. The patient demographics and clinical characteristics are summarized in Supplementary Table 2 (available online) (20). RNA isolation, cDNA conversion, quantitative polymerase chain reaction (qPCR), and gene expression analysis were performed as described in the Supplementary Methods and Supplementary Table 3 (available online). Because of the small number of women in the study population, we did not report subanalyses by sex, but analysis by major racial/ethnic group was done.

### In Vivo Studies

Animal care and experimental procedures were approved by the Institutional Animal Care and Use Committee, Biological Resource Centre, Agency for Science, Technology and Research (A*STAR), Singapore. The spontaneous liver tumor mouse model and transplanted tumor mouse model are described in the Supplementary Methods (available online).

### Immunohistochemistry

Paraffin-embedded tissue sections of liver and tumor from HCC patients (n = 40) or from mice used in the above experiments were processed as previously described (4). All the antibodies used are listed in Supplementary Table 1 (available online). A terminal deoxynucleotidyl transferase dUTP nick end labeling kit from Millipore (Billerica, MA) was used as per the manufacturer's protocol. Immunohistochemistry (IHC) images were captured with a DP20 camera attached to a CX31 microscope (Olympus, Center Valley, PA). For immunoflourescence images, an Olympus FlourView FV1000 confocal microscope was used. The number of positively stained cells in 10–12 random fields were counted at ×100 magnification using Image-Pro Analyzer version 6.2 (Media Cybernetics, Inc, Rockville, MD).

### Flow Cytometry

Apoptotic HCC cells were identified by staining with Annexin V (BD Pharmingen, San Diego, CA) and Topro-3 (Invitrogen). Activation of $CD56^+$ human NK cells was determined by assessing the protein expression of the early activation marker CD69 using antihuman CD69 antibody (eBiosciences, San Diego, CA). Immune cells were isolated from mouse liver tumors or healthy livers by digesting the tissues with Collagenase A (1 mg/mL) and DNase I (0.1 mg/mL; Roche, Indianapolis, IN) and were analyzed using antibodies listed in Supplementary Table 1 (available online). All flow cytometry analyses were done on a BD LSRII flow cytometer equipped with five lasers (BD Biosciences, San Jose, CA), and the data were processed using FlowJo version 7.5 software (Tree Star, Inc, Ashland, OR).

### NK-Cell Activation and Cytotoxicity Assay

Blood samples from 15 healthy donors were obtained from the Singapore Health Science Authority blood bank following Ethics Committee approval. NK cells were isolated by negative selection using the NK-cell isolation kit (Miltenyi Biotec, Bergisch Gladbach, Germany), treated, and analyzed by using the DELFIA EuTDA-based cytotoxicity assay kit (Perkin-Elmer, Boston, MA) by following the manufacturer's instructions (Supplementary Methods, available online). IFN-γ present in supernatants from activated NK cells was measured by enzyme-linked immunosorbent assay (Biolegend, San Diego, CA) by following the manufacturer's instructions.

### Statistical Analysis

Kaplan–Meier univariate survival analysis was performed using data from HCC patients and hazard ratios (HRs), 95% confidence intervals (CIs), and *P*-values were calculated using the log-rank (Mantel–Cox) test. Paired or unpaired *t*-tests, Mann–Whitney tests, or one- or two-way analysis of variance tests were also used in various experiments as indicated. A *P*-value less than .05 was considered statistically significant. All statistical tests were two-sided. For more detailed information on the statistical analyses, see the Supplementary Methods (available online).

## Results

### TLR3 Expression in Tumor Parenchyma and Infiltrating NK Cells in HCC Patient Samples

We previously reported that *TLR3* gene expression in tumors was associated with overall survival among a cohort of 61 patients from Singapore (4). Here, we extended our previous study to include 111 additional patients from Hong Kong and Zurich. First, we performed qPCR on patient samples and confirmed that expression of *TLR3* is associated with overall survival (HR of survival = 2.1, 95% CI = 1.3 to 3.4, *P* = .002) (Figure 1, A). We also observed

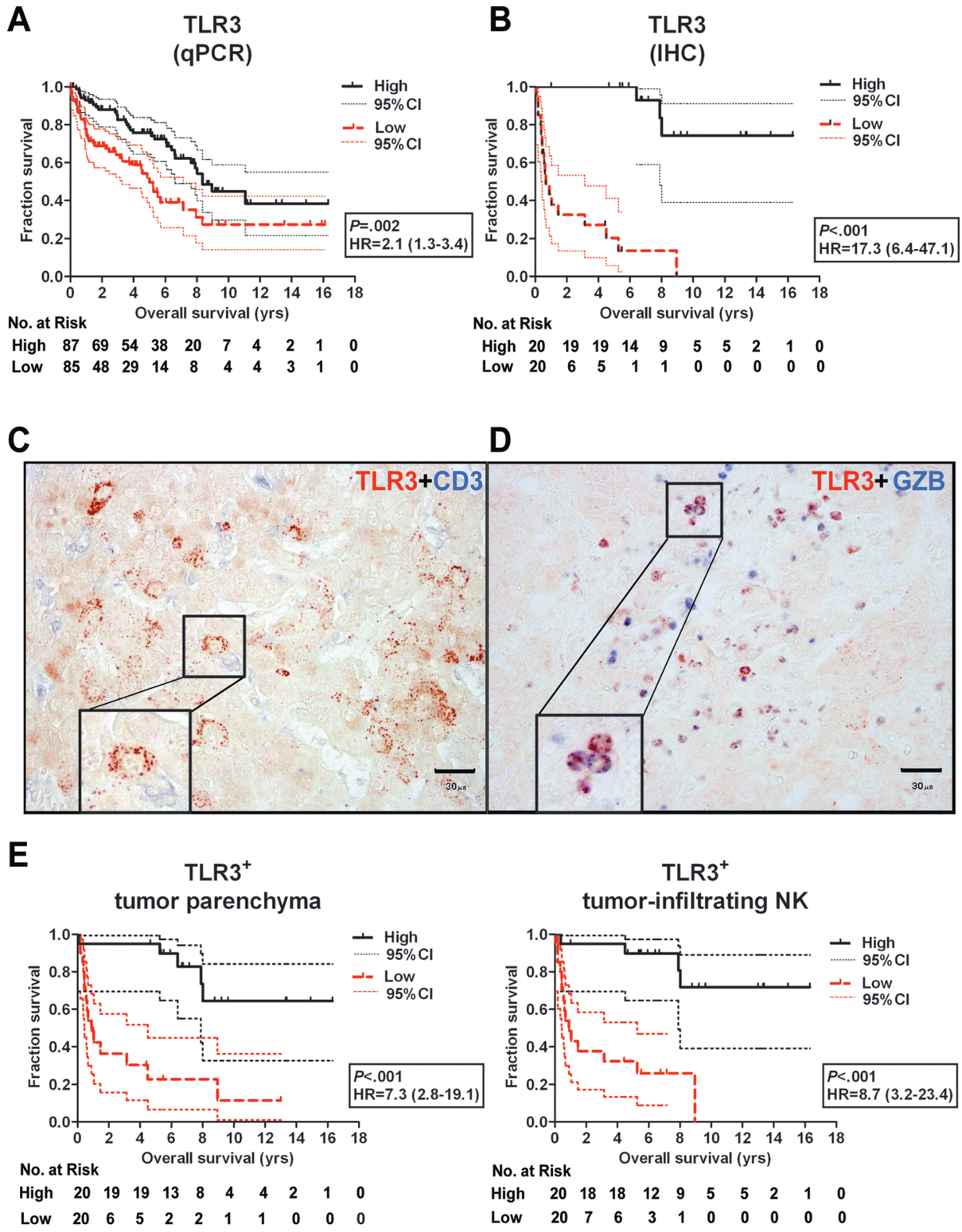


**Figure 1.** The association of intratumor toll-like receptor 3 (TLR3) expression by tumor parenchyma and natural killer (NK) cells with patient survival. Kaplan–Meier analyses were done to investigate the association between **A**) *TLR3* gene expression (by quantitative polymerase chain reaction, n = 172) and **B**) TLR3 protein levels (by immunohistochemistry [IHC], n = 40, median = 33 cells per field) and patient survival. Log-rank Mantel–Cox test was used to calculate two-sided *P*-values. Representative IHC images at ×400 magnification of **C**) TLR3$^+$ tumor parenchyma (**red** indicates TLR3 staining and **blue** indicates CD3 staining) and **D**) TLR3$^+$ NK cells (**red** indicates TLR3 staining; NK cells are identified by granzyme-B expression in **blue**; and costaining appears **purple**) are shown. The insets show magnified areas. **Scale bar** = 30 μm. **E**) Kaplan–Meier analyses of TLR3$^+$ tumor cell (median = 21 cells per field) and tumor-infiltrating NK cells densities (median = 13 cells per field) and patient survival (n = 40). The log-rank Mantel–Cox test was used to calculate two-sided *P*-values. CI = confidence interval, HR = hazard ratio.

a statistically significant association using IHC to analyze TLR3 protein expression in 40 representative tumor samples (HR of survival = 17.3, 95% CI = 6.4 to 47.1, $P < .001$) (Figure 1, B). TLR3 was either expressed by tumor parenchyma (Figure 1, C) or small round immune cells infiltrating the tumor nest (Figure 1, D). TLR3 was coexpressed with granzyme B but not with CD3 or CD20, suggesting that the cells that stained positively for TLR3 were NK cells (Figure 1, D) and not T or B cells (Supplementary Figure 1, available online). We next quantified TLR3 expression separately in tumor parenchyma (hepatocytes) and NK cells to determine if these two cell populations were associated with overall survival. As shown in Figure 1, E, both TLR3-expressing cell populations were associated with overall survival in Kaplan–Meier analyses (tumor parenchyma: HR of survival = 7.3, 95% CI = 2.8 to 19.1, $P < .001$; tumor-infiltrating NK cells: HR of survival = 8.7, 95% CI = 3.2 to 23.4, $P < .001$).

### Effect of TLR3 Activation on HCC Cell Death

To study the effects of endogenous expression of TLR3 in HCC, we screened 11 human HCC cell lines for *TLR3* RNA expression by qPCR and identified seven—SNU182, SNU387, SNU449, SNU475, SK-HEP-1, HepG2, and Hep3B—that expressed the receptor (data not shown). Treatment of SNU182 cells, which exhibited high expression of *TLR3*, with increasing concentration of poly(I:C) for 24 hours at 37°C, resulted in a dose-dependent increase in cell death (no treatment vs 50 µg/mL poly(I:C): 8.5% vs 30.5%, $P = .03$; no treatment vs 100 µg/mL poly(I:C): 8.5% vs 30.9%, $P = .03$) (Figure 2, A). Similar results were observed for SNU449 and SNU475 cells that express moderate levels of TLR3 (Supplementary Figure 2, A, available online). TLR3 expression was increased in a dose-dependent manner by treatment with poly(I:C) in SNU182 cells (Supplementary Figure 2, B, available online). Ligands for other TLRs (lipopolysaccharide and CpG) did not induce cell death in SNU182 cells (Supplementary Figure 2, C, available online), and no effect was observed in PLC/PR5 cells that do not express *TLR3* (Supplementary Figure 2, D, available online). In addition, knock-down of *TLR3* in SNU182 cells reduced poly(I:C)-induced cell death (scrambled vs TLR3 siRNA: 39.9% vs 27.2%, $P = .03$) (Figure 2, B, and Supplementary Figure 2, E, available online). As poly(I:C) is a ligand for both TLR3 and MDA5 (21), we treated the cells with the TLR3-specific ligand poly(A:U) and observed similar results (Supplementary Figure 2, F, available online). These data indicate that TLR3 activation induces cell death in HCC cells that express endogenous TLR3.

### Effect of TLR3 Activation on NK-Cell Activation and Cytotoxicity Against HCC Cells

We next evaluated the antitumor properties of NK cells following TLR3 activation. NK-cell treatment with poly(I:C) led to a marked increase in expression of the early activation marker CD69 [percentage of $CD56^+CD69^+$ cells relative to all live $CD45^+$ cells after poly(I:C) treatment vs control = 32.6% vs 19.4%, $P < .001$] (Figure 3, A) and in expression of cytotoxic mediators, such as IFN-γ [ninefold increase in *IFNG* gene expression after treatment with poly(I:C), $P < .001$; mean secreted IFN-γ after treatment with poly(I:C) vs control = 415 vs 179 pg/mL, $P = .03$] (Figure 3, B and C) and granzyme-B [threefold increase in granzyme-B gene expression after treatment with poly(I:C), $P < .001$] (Figure 3, B). Activated NK cells displayed up to fourfold higher cytotoxic activity (E:T ratio = 5:1, $P = .03$) against SNU182 cells (Figure 3, D). Thus, in vitro activation of TLR3 promotes NK-cell activation, secretion of IFN-γ, and cytotoxicity against HCC cells. This result is consistent with previous studies using lymphoma target cells (19).

### Effect of TLR3 Activation on Intratumoral Chemokine Expression and NK-Cell Infiltration

To investigate the effect of TLR3 activation in vivo, we treated mice that spontaneously develop liver tumors with poly(I:C) (22,23). In the tumors of treated mice compared with mice injected with PBS or livers from age-matched, tumor-free mice, increase in relative expression of the chemokine genes *Ccl5* (HCC of tumor-bearing mice treated with poly(I:C) vs PBS = 19-fold increase, $P = .01$; vs livers of tumor-free mice = 189-fold increase, $P = .02$) and *Cxcl9* (HCC of tumor-bearing mice treated with poly(I:C) vs PBS = fivefold increase, $P = .04$; vs livers of tumor-free mice = 12-fold increase, $P = .04$) was observed (Figure 4, A). CCL5 and CXCL9 proteins were expressed by both the tumor-infiltrating leukocytes (TILs) and tumor parenchymal cells (Supplementary Figure 3, A, available online). Further studies on TILs revealed expression of CCL5 by T cells and macrophages and CXCL9 expression by macrophages (Supplementary Figure 3, B, available online). These results are consistent with our previous data from human HCC samples (20). Furthermore, poly(I:C) treatment induced NK-cell infiltration [percentage of NK $1.1^+$ cells relative to all live $CD45^+$ cells in HCC of tumor-bearing mice treated with poly(I:C) vs PBS or livers of tumor-free mice = 14.6% vs 4%, $P = .002$ or 4.2%, $P = .02$, respectively] (Figure 4, B) and stimulated expression of the NK-cell effector genes *Prf* and *Gzmb* [13-fold increase in mean relative expression of *Prf* in poly(I:C) vs PBS-treated mice, $P = .03$, and 29-fold increase in mean relative expression of *Gzmb* in poly(I:C) vs PBS-treated mice, $P < .001$] (Figure 4, C). Increased intratumor expression of *Tlr3* was also observed in these mice (Supplementary Figure 3, C, available online), in agreement with the in vitro data presented in Supplementary Figure 2, C (available online). No statistically significant difference was observed in the numbers of tumor-infiltrating T cells or macrophages, or in the expression of *Ccl2* or *Cxcl10* genes (Supplementary Figure 3, D and E, available online). Treating the mice with poly(A:U) also increased NK-cell infiltration and chemokine expression in the liver tumors (Supplementary Figure 4, A and B, available online).

The effect of intratumor expression of CCL5 and CXCL9 (24) was further studied in C57BL/6J mice transplanted subcutaneously with the mouse HCC cell line Hepa1-6. Expression of these two chemokines increased intratumor lymphocyte infiltration (fourfold increase in mean relative expression of *Cd3g* in tumor cells transfected with *Ccl5/Cxcl9* vs control (Ctl), $P = .009$) (Supplementary Figure 5, A, available online) and slowed down tumor growth (mean tumor area of *Ccl5/Cxcl9* transfected vs control groups = 9.2 vs 22.0 $mm^2$, $P = .02$ on day 7; 11.7 vs 26.5 $mm^2$, $P = .006$ on day 10; and 15.8 vs 39.5 $mm^2$, $P < .001$ on day 14) (Supplementary Figure 5, B, available online). When NK cells were depleted using PK136 antibody, tumor growth was enhanced (mean tumor area of PK136 vs isotype control treated groups = 42.3 vs 18.7 $mm^2$, $P = .005$ on day 7; 44.3 vs 16.0 $mm^2$, $P < .001$ on day 10; and 56.3 vs 23.3 $mm^2$,

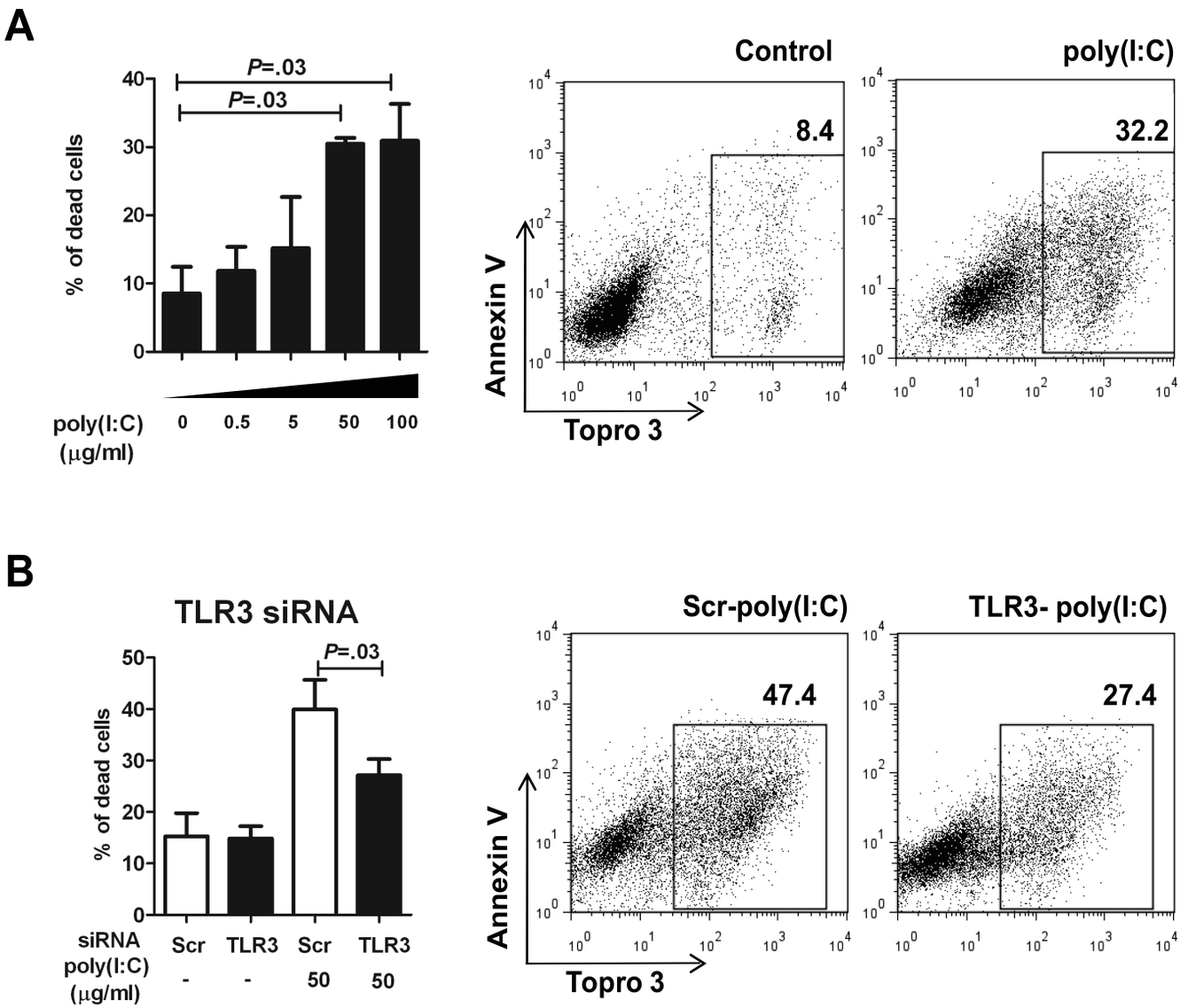


**Figure 2.** The effect of toll-like receptor 3 (TLR3) activation by poly(I:C) on hepatocellular carcinoma cell line death. **A**) Dose-dependent induction of cell death in SNU182 cells was measured as Annexin V$^+$ Topro 3$^+$ cells by flow cytometry 24 hours after treatment with 0–100 μg/mL poly(I:C). The graph shows the means and SD from three independent experiments. A one-way analysis of variance test with Tukey's multiple comparison post test was used to calculate two-sided *P*-values. In the right panel, representative dot plots of cell death 24 hours post-treatment with 50 μg/mL poly(I:C) are shown. **B**) Poly(I:C)-induced cell death (Annexin V$^+$ Topro 3$^+$ cells by flow cytometry) in SNU182 cells with TLR3 or scrambled siRNA knockdown was measured 24 hours after treatment with 50 μg/mL poly(I:C). The graphs show the means and SD from three independent experiments. Unpaired *t*-test was used to calculate two-sided *P*-values. The right panel shows representative dot plots of poly(I:C)-induced cell death with TLR3 knockdown. Scr = scrambled siRNA.

$P < .001$ on day 14) (Figure 4, D), further demonstrating the critical role of NK cells in controlling HCC tumor growth.

### Effect of TLR3 Activation In Vivo on Intratumor Proliferation of T Cells and NK Cells and Viability of Tumor Parenchyma

We next characterized the functional status of TILs in poly(I:C)-treated mice. As shown in Figure 5, A, the frequency of Ki67$^+$CD45$^+$ proliferating TILs was ninefold higher in liver tumors from poly(I:C)- vs PBS-treated mice (mean number of Ki67$^+$CD45$^+$ TILs per field = 167 vs 19, respectively, $P < .001$). Furthermore, double-IHC using antibodies against Ki67 with either CD3 or granzyme B identified these proliferating TILs as T cells and NK cells (Figure 5, B). Conversely, proliferation of tumor parenchyma cells (identified as Ki67$^+$CD45$^-$ cells with distinct morphology) was fourfold lower in poly(I:C)- vs PBS-treated mice (mean = 41 vs 166 cells per field, respectively, $P = .002$) (Figure 5, C), whereas apoptosis of tumor cells was enhanced by 11-fold (mean = 32 vs 3 cells per field, respectively, $P < .001$) (Figure 5, D). Similar results were observed when mice were treated with poly(A:U) (Supplementary Figure 4, C and D, available online). These data show that TLR3 activation in tumor-bearing mice increased the proliferation of tumor-infiltrating T and NK cells whereas tumor-cell proliferation and viability were decreased.

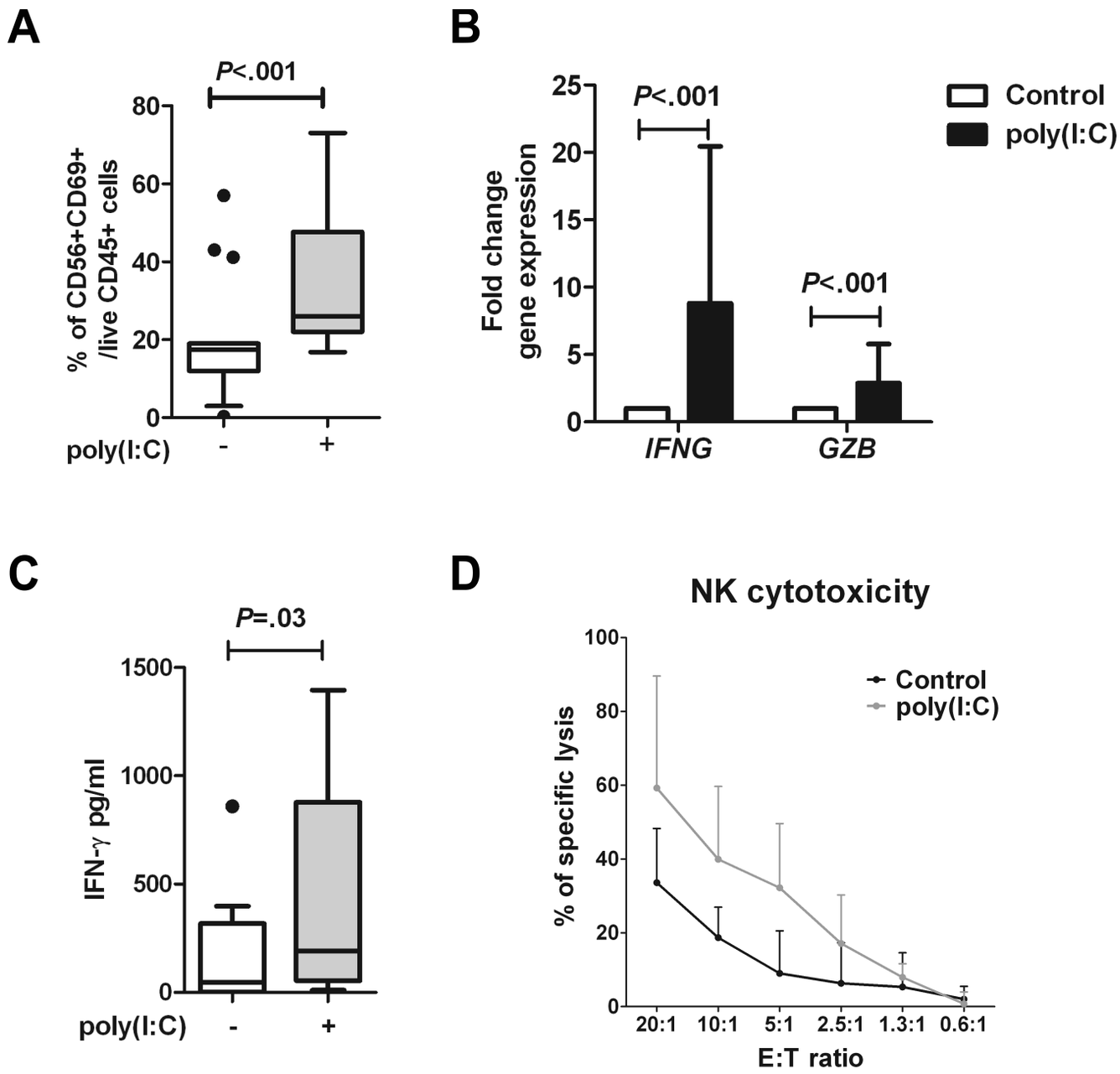


**Figure 3.** The effect of toll-like receptor 3 (TLR3) activation on natural killer (NK)-cell activation and cytotoxicity against hepatocellular carcinoma cells in vitro. **A**) The percentage of activated NK cells coexpressing CD56 with the early activation marker CD69 was measured by flow cytometry 24 hours after treatment with 50 μg/mL poly(I:C). Data are shown using Tukey box-and-whiskers representation from 15 independent experiments. A paired *t*-test was used to calculate the two-sided *P*-value. **B**) Expression of the effector genes interferon-γ (*IFNG)* and granzyme-B (*GZB)* was determined by quantitative polymerase chain reaction 24 hours after NK cells were treated with 50 μg/mL poly(I:C). The graph shows the mean fold change relative to the untreated control from 12 independent experiments. **Whisker bars** indicate the SD. A Wilcoxon signed-rank test was used to calculate the two-sided *P*-values. **C**) The mean interferon-γ (IFN-γ) secretion by NK cells 24 hours after treatment with 50 μg/mL poly(I:C) was measured by enzyme-linked immunosorbent assay of the culture supernatant. The data are shown using Tukey box-and-whiskers representation from eight independent experiments. A paired *t*-test was used to calculate the two-sided *P*-value. **D**) Cytotoxicity of poly(I:C)-activated NK cells at various ratios of effector (E) to target cells (T, SNU182 cells) was measured by determining the percentage of specific lysis in vitro. A paired *t*-test was used to calculate the two-sided *P*-value at E:T ratio of 5:1. The graph shows the means from poly(I:C)-treated and untreated NK cells and the SD (**whisker bars**) from three independent experiments.

To further show the effect of TLR3 in controlling tumor growth, we treated C57BL/6J mice transplanted with Hepa1-6 cells with poly(I:C) and observed a statistically significant reduction in tumor growth compared with PBS-treated mice (mean tumor area of poly(I:C)- vs PBS-treated mice = 14.5 vs 39.5 $mm^2$, $P < .001$, day 14) (Figure 5, E). Infiltration of T cells and NK cells was also increased in transplanted tumors from the poly(I:C)-treated mice (T-cell infiltration: threefold increase in mean relative expression of *Cd3g*, $P = .01$; NK-cell infiltration: twofold increase in mean relative expression of *Nkp46*, $P = .04$) (Figure 5, F).

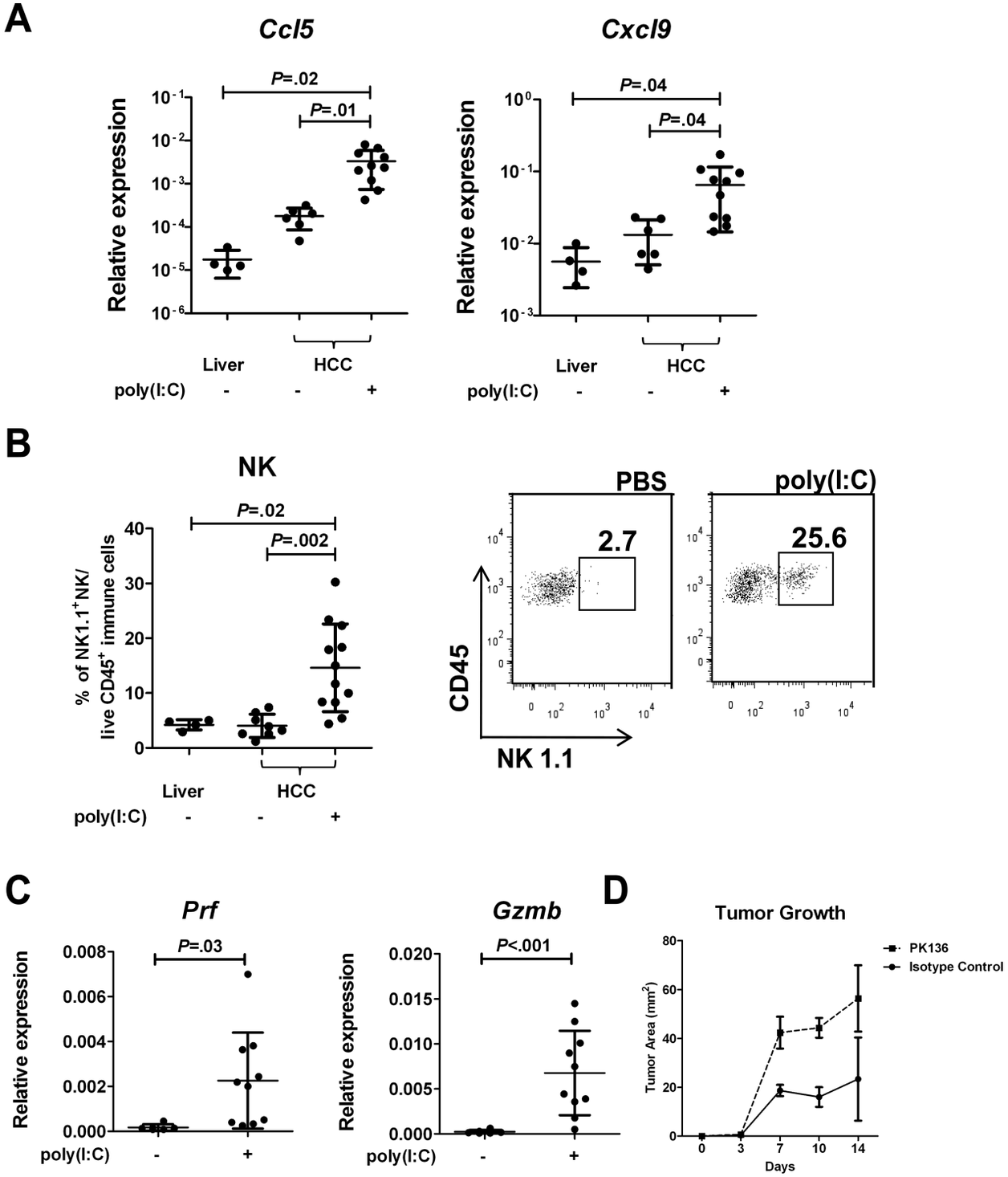


**Figure 4.** The effect of toll-like receptor 3 (TLR3) activation on intratumor chemokine expression and natural killer (NK)-cell infiltration in hepatocellular carcinoma in vivo. **A**) The mean RNA expression of the *Ccl5* and *Cxcl9* chemokines in liver tumors from mice treated with poly(I:C) (n = 6), or phosphate buffered saline (PBS)-treated mice (n = 4), or livers from non-tumor-bearing littermates (n = 2), is shown. **Whisker bars** indicate the SD. A one-way analysis of variance test with Bonferroni correction was used to calculate the two-sided *P*-values. **B**) In the left panel, the mean percentage of NK1.1$^+$ CD45$^+$ NK-cell infiltration of liver tumors harvested from poly(I:C)-treated mice (n = 6), or PBS-treated mice (n = 4), or livers from non-tumor-bearing littermates (n = 2), is shown. **Whisker bars** indicate the SD. A one-way analysis of variance test with Bonferroni correction was used to calculate the two-sided *P*-values. In the right panel, representative dot plots showing the percentage of NK1.1$^+$ CD45$^+$ NK cells (box) infiltrating the liver tumors harvested from poly(I:C)- and PBS-treated mice. **C**) The mean expression of the NK-cell effector genes perforin (*Prf*) and granzyme-B (*Gzmb*) was measured in liver tumors harvested from poly(I:C)- and PBS-treated mice using quantitative polymerase chain reaction. Graphs show means and SD. The Mann–Whitney test was used to calculate the two-sided *P*-values. **D**) Transplanted tumor growth was measured after NK cells were depleted using PK136 antibody or isotype control antibody (n = 3 per group). The graphs show the means and SD (**whisker bars**). A two-way analysis of variance test with Bonferroni correction was used to calculate two-sided *P*-values. The mean tumor area was statistically significantly different between PK136-treated and isotype control–treated mice at days 7, 10, and 14 ($P = .005$, <.001, and <.001, respectively).

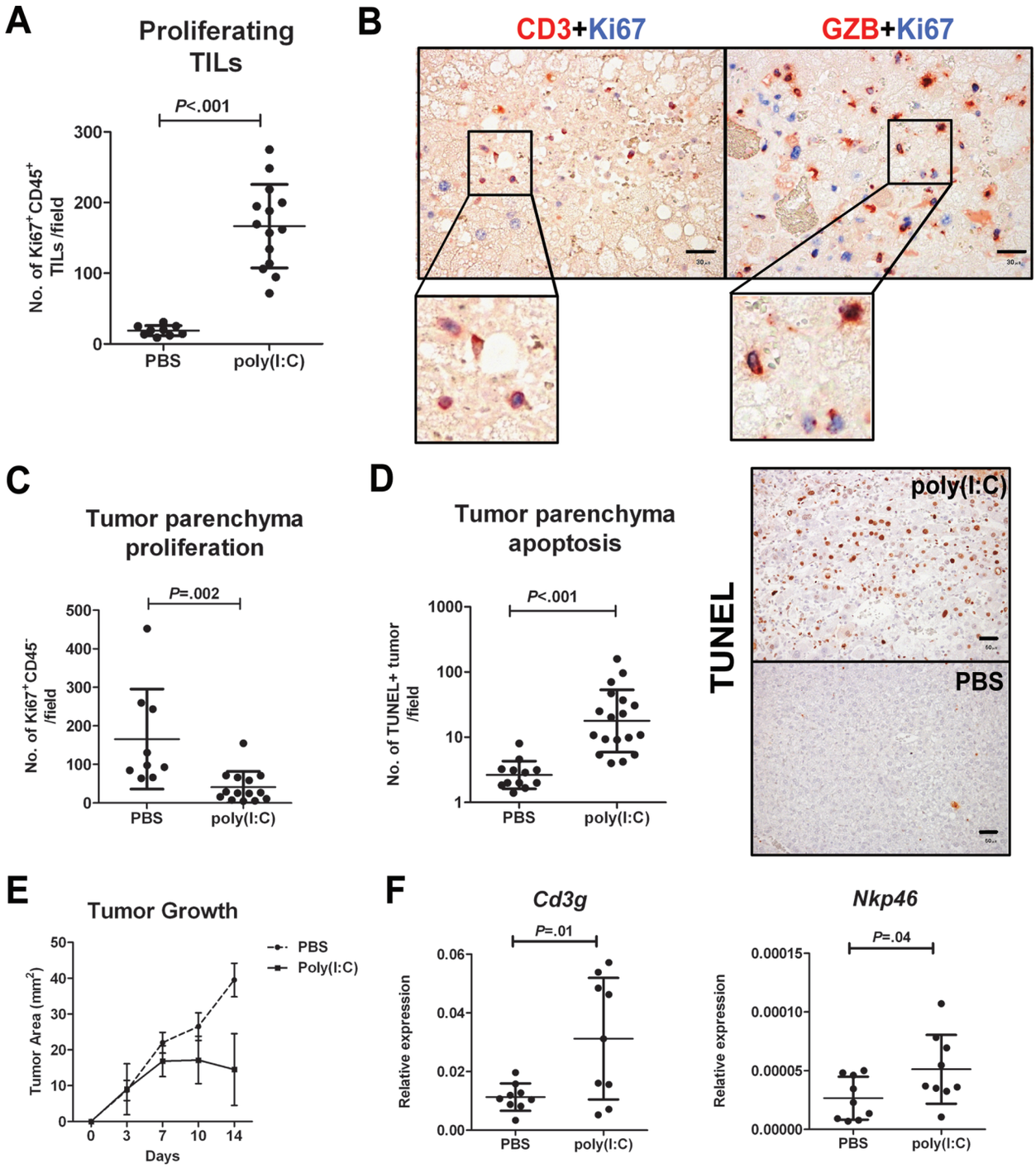


**Figure 5.** The effect of toll-like receptor 3 (TLR3) activation on antitumor activity in vivo. **A**) The mean number of $Ki67^+CD45^+$ proliferating tumor-infiltrating leukocytes per field was assessed by immunohistochemistry in liver tumors from poly(I:C)-treated mice compared with phosphate buffered saline (PBS)-treated mice. **Whisker bars** indicate the SD. An unpaired *t*-test was used to calculate the two-sided *P*-value. **B**) Representative immunohistochemical images of CD3 or granzyme-B (GZB) staining (**red**) and Ki67 (**blue**) at ×400 magnification. Membrane expression of CD3, cytoplasmic expression of GZB, and nuclear expression of Ki-67 were observed. The insets show a representative magnified area. **Scale bar** = 30 μm. **C**) The mean number of $Ki67^+CD45^-$ proliferating tumor parenchyma cells per field in liver tumors harvested from poly(I:C)-treated mice compared with PBS-treated mice is shown. **Whisker bars** indicate the SD. The Mann–Whitney test was used to calculate the two-sided *P*-value. **D**) The mean number of apoptotic tumor parenchyma cells per field detected by terminal deoxynucleotidyl transferase dUTP nick end labeling in liver tumors harvested from poly(I:C)-treated or PBS-treated mice is shown. **Whisker bars** indicate the SD. The Mann–Whitney test was used to calculate the two-sided *P*-value. Representative immunohistochemical images are also shown at ×200 magnification. **Scale bar** = 50 μm. **E**) Transplanted tumor growth was determined in mice treated with poly(I:C) vs PBS (n = 6 mice per group). On day 14, the mean tumor area of poly(I:C)- vs PBS-treated mice is 14.5 vs 39.5 $mm^2$, $P < .001$. **Whisker bars** indicate the SD. A two-way analysis of variance test with Bonferroni correction was used to calculate the two-sided *P*-value. **F**) Relative gene expression of T (threefold increase in *Cd3g*) and NK (twofold increase in *Nkp46*) cell markers in transplanted tumors treated with poly(I:C) vs PBS (n = 6 mice per group) is shown. The graphs show the means and SD (**whisker bars**). An unpaired *t*-test was used to calculate the two-sided *P*-values.

### Correlation Between TLR3, NK-Cell Infiltration, and Antitumor Activity in Patient Samples

In tumor tissue from HCC patients, a higher density of TLR3-expressing cells correlated with increased tumor infiltration by $CD56^+$ NK cells (Pearson's $r = 0.7$, $P < .001$) and $CD8^+$ T cells (Pearson's $r = 0.6$, $P < .001$) (Figure 6, A). This is consistent with our previous finding that *TLR3* RNA expression is associated with expression of chemokines able to attract NK cells and T cells (20). Furthermore, TLR3 protein expression correlated with NK-cell activation marker *IFNG* expression when measured by qPCR (Pearson's $r = 0.5$, $P = .001$), and a similar, albeit weaker, correlation was observed with granzyme-B expression when measured by IHC (Pearson's $r = 0.4$, $P = .03$) (Figure 6, B). Correlations between *TLR3* and *NCR3*, *CD8A*, and *IFNG* (NK- and T-cell marker) were also observed at the RNA level in patient samples (n = 154–164) (Supplementary Table 4, available online). In addition, the density of both $TLR3^+$ tumor parenchyma and NK cells correlated positively with tumor cell apoptosis ($TLR3^+$ tumor parenchyma, Pearson's $r = 0.5$, $P = .006$; $TLR3^+$ NK cells, Pearson's $r = 0.6$, $P = .002$) and negatively with tumor cell proliferation ($TLR3^+$ tumor parenchyma, Pearson's $r = -0.4$, $P = .03$; $TLR3^+$ NK cells, Pearson's $r = -0.5$, $P = .005$) (Figure 6, C) and were decreased in samples from patients with stage III and IV advanced HCC (Supplementary Figure 6, available online). These data from HCC patients are consistent with our in vitro and in vivo findings that TLR3 activation is associated with intratumor expression of chemokines, NK- and T-cell infiltration, NK-cell activation, and antitumor activity, as well as enhanced apoptosis and reduced proliferation of tumor parenchyma cells.

## Discussion

In the past few decades, TLR agonists have emerged as promising drugs for the treatment of cancer (25). Several TLR ligands have since been used to treat cancer patients either as a monotherapy or in combination with other therapies (17). These ligands include the TLR7 ligand imiquimod for superficial basal cell carcinoma (26) and the TLR9 ligand CpG ODN for a variety of carcinomas (27). In particular, TLR3 ligands were used to treat patients with various malignancies, including breast cancer (28) and melanoma (29). We previously showed that TLR3 expression is associated with superior HCC patient survival (4). Here, we confirmed this finding using a larger set of patient samples and explored the underlying mechanisms of the beneficial role of TLR3 activation in HCC.

By integrating in vitro data from human cell lines with in vivo treatment of mice that developed spontaneous HCC or were injected with HCC cell line, we demonstrated that the prolonged survival associated with higher expression of TLR3 may result from three independent effects: induction of tumor parenchyma (hepatocytes) cell death; induction of intratumor expression of chemokines that attract NK cells or T cells to the tumor microenvironment; and activation of tumor-infiltrating NK cells that promote cytotoxic activity. These effects were consistent with transcriptomal and histopathological analyses of HCC patient samples.

TLR3 is expressed by tumor parenchyma and infiltrating NK cells. We showed that expression in both compartments correlated with reduced tumor cell proliferation, increased tumor cell death, and prolonged patient survival. TLR3 expression by tumor parenchyma was associated with improved survival even in patients with low *NCR3* expression (Kaplein–Meier analysis, HR of survival = 7.1, 95% CI = 1.7 to 30.5, $P = .008$) (unpublished data), indicating that TLR3 expression has independent effects on the tumor parenchyma and infiltrating NK cells. Moreover, during disease progression (from stages I and II to stages III and IV), TLR3 expression is downregulated in both compartments, suggesting that expression of TLR3 in both cell populations impacts on patient survival. These findings are consistent with our in vitro data; TLR3 activation induces apoptosis and chemokine expression in tumor and also stimulates the functional activation of NK cells. Patients with high TLR3 expression are found in both early and late stage groups ($P = .56$) (unpublished data), suggesting that earlier diagnosis of HCC in these patients is unlikely to explain their prolonged survival.

In vitro activation of TLR3 was previously reported to trigger apoptosis in several tumor cell lines, including breast cancer (10), melanoma (11), and even HCC cell lines transfected with TLR3 (18,30). $TLR3^+$ NK cells are directly activated by treatment with poly(I:C) (6,19,31). Previous studies from prostate and glioma tumor models showed that TLR3 activation enhanced chemokine expression and immune effector cell infiltration. Both studies suggest that TLR3-induced immune infiltration promotes antitumor activity. Our study confirms and expands on these previous reports by providing in vitro and in vivo evidence on the multiple mechanisms of TLR3-mediated HCC progression. The effects of TLR3 activation observed in our study are consistent with a previous study in breast cancer showing that only patients with $TLR3^+$ tumors benefited from poly(A:U) treatment (28).

We showed that TLR3 activation enhances intratumor expression of chemokines that attract NK cells and stimulates IFN-γ production by NK cells. IFN-γ is known to synergize with inflammatory cytokines, such as TNF-α, to further induce expression of NK cell–attracting chemokines (20,32). This synergy could lead to further tumor infiltration by NK cells through a positive paracrine loop. In addition, HCC cells killed by NK cells may release TLR ligands that further activate NK cells to trigger more parenchyma cell death, thus amplifying antitumor activity. These putative feedback loops will require further investigation to establish whether they can account for the strong association between TLR3 expression and prolonged HCC patient survival.

In HCC patients, we observed a correlation between intratumor expression of TLR3 and the density of tumor-infiltrating $CD8^+$ T cells, whereas treating tumor-bearing mice with poly(I:C) failed to increase T-cell infiltration in liver tumors. This discrepancy could be attributed to the analysis of murine tumors only 3 days after treatment, which could be an insufficient time period for T cells to expand and accumulate. In patients, however, sustained signaling through TLR3 may lead to increased recruitment and proliferation of T cells. In the transplanted HCC tumor model, poly(I:C) promoted tumor infiltration by both NK and T cells at day 16.

Our study has several limitations. First, the effect of poly(I:C) on tumor growth was only analyzed in a transplanted, nonorthotopic model of HCC. In the spontaneous orthotopic model, in which

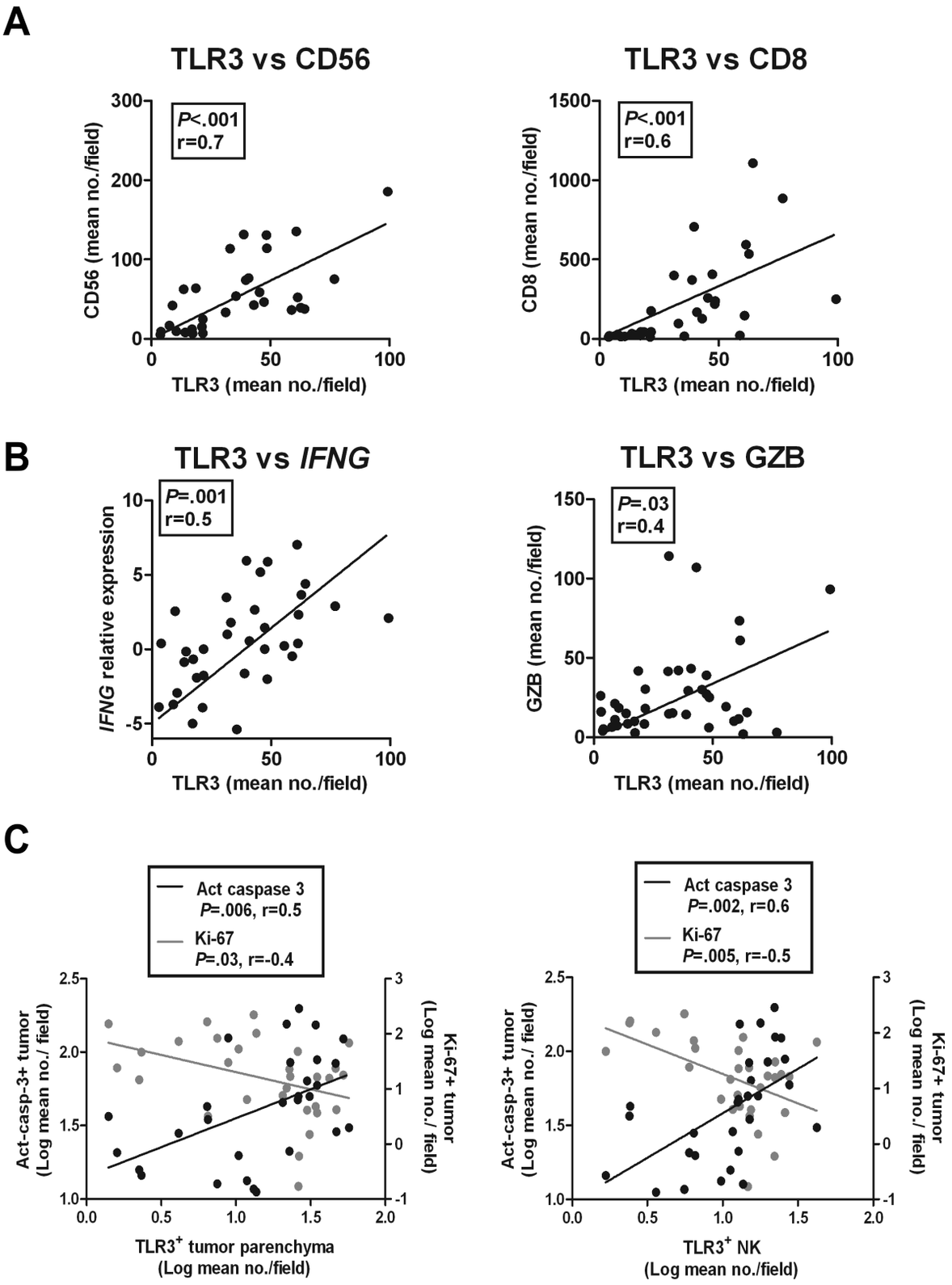


**Figure 6.** The correlation between toll-like receptor (TLR3) expression and tumor infiltration by natural killer (NK) cells and antitumor activity in hepatocellular carcinoma patients. **A**) The density of TLR3$^+$ cells correlates with the density of CD56$^+$ NK and CD8$^+$ T cells in patient samples as determined by immunohistochemistry (n = 31). **B**) The density of TLR3$^+$ cells correlates with RNA expression of interferon-γ (*IFNG*, n = 35) and with the density of granzyme-B (GZB)-positive cells by immunohistochemistry (n = 40) in hepatocellular carcinoma patient samples. **C**) The density of TLR3$^+$ tumor parenchyma and tumor-infiltrating NK cells correlates positively with the density of Ki-67$^+$ tumor parenchyma cells, and negatively with the density of activated caspase 3$^+$ tumor parenchyma cells (n = 30). The Pearson correlation test was used to calculate the correlation coefficient (*r*) and two-sided *P*-values.

tumors take months to develop, we only treated the tumors with poly(I:C) for a short time. In addition, the effect of poly(I:C) on human NK cells was assessed only with cells from healthy donors, and future studies are required to show that patient NK cells are functionally identical. Finally, not all HCC cell lines undergo apoptosis after TLR3 triggering, and the molecular basis of this variation is not known.

In summary, our study shows that TLR3 expression by tumor parenchyma and infiltrating NK cells was associated with superior HCC patient survival. TLR3 is likely to act directly on tumor parenchyma cells and promote the recruitment and activation of NK cells. Several synergistic pathways involving chemokines and IFN-γ or release of TLR ligands by dying cells may reinforce these effects. These findings emphasize the need for further clinical studies aimed at evaluating the potential of TLR3 ligands to treat HCC.

## References


1. Llovet JM, Burroughs A, Bruix J. Hepatocellular carcinoma. *Lancet*. 2003;362(9399):1907–1917.
2. Kremsdorf D, Soussan P, Paterlini-Brechot P, Brechot C. Hepatitis B virus-related hepatocellular carcinoma: paradigms for viral-related human carcinogenesis. *Oncogene*. 2006;25(27):3823–3833.
3. Nakamoto Y, Guidotti LG, Kuhlen CV, Fowler P, Chisari FV. Immune pathogenesis of hepatocellular carcinoma. *J Exp Med*. 1998;188(2):341–350.
4. Chew V, Tow C, Teo M, et al. Inflammatory tumour microenvironment is associated with superior survival in hepatocellular carcinoma patients. *J Hepatol*. 2010;52(3):370–379.
5. Matsumoto M, Funami K, Tanabe M, et al. Subcellular localization of Toll-like receptor 3 in human dendritic cells. *J Immunol*. 2003;171(6):3154–3162.
6. Pisegna S, Pirozzi G, Piccoli M, Frati L, Santoni A, Palmieri G. p38 MAPK activation controls the TLR3-mediated up-regulation of cytotoxicity and cytokine production in human NK cells. *Blood*. 2004;104(13):4157–4164.
7. Farina GA, York MR, Di Marzio M, et al. Poly(I:C) drives type I IFN- and TGFβ-mediated inflammation and dermal fibrosis simulating altered gene expression in systemic sclerosis. *J Invest Dermatol*. 2010;130(11):2583–2593.
8. Guillot L, Le Goffic R, Bloch S, et al. Involvement of toll-like receptor 3 in the immune response of lung epithelial cells to double-stranded RNA and influenza A virus. *J Biol Chem*. 2005;280(7):5571–5580.
9. Li K, Chen Z, Kato N, Gale M Jr, Lemon SM. Distinct poly(I-C) and virus-activated signaling pathways leading to interferon-beta production in hepatocytes. *J Biol Chem*. 2005;280(17):16739–16747.
10. Salaun B, Coste I, Rissoan MC, Lebecque SJ, Renno T. TLR3 can directly trigger apoptosis in human cancer cells. *J Immunol*. 2006;176(8):4894–4901.
11. Salaun B, Lebecque S, Matikainen S, Rimoldi D, Romero P. Toll-like receptor 3 expressed by melanoma cells as a target for therapy? *Clin Cancer Res*. 2007;13(15, pt 1):4565–4574.
12. Matsumoto M, Funami K, Oshiumi H, Seya T. Toll-like receptor 3: a link between toll-like receptor, interferon and viruses. *Microbiol Immunol*. 2004;48(3):147–154.
13. Beg AA. Endogenous ligands of Toll-like receptors: implications for regulating inflammatory and immune responses. *Trends Immunol*. 2002;23(11):509–512.
14. Marshak-Rothstein A. Toll-like receptors in systemic autoimmune disease. *Nat Rev Immunol*. 2006;6(11):823–835.
15. Salem ML, Kadima AN, Cole DJ, Gillanders WE. Defining the antigen-specific T-cell response to vaccination and poly(I:C)/TLR3 signaling: evidence of enhanced primary and memory CD8 T-cell responses and antitumor immunity. *J Immunother*. 2005;28(3):220–228.
16. Schulz O, Diebold SS, Chen M, et al. Toll-like receptor 3 promotes cross-priming to virus-infected cells. *Nature*. 2005;433(7028):887–892.
17. Adams S. Toll-like receptor agonists in cancer therapy. *Immunotherapy*. 2009;1(6):949–964.
18. Khvalevsky E, Rivkin L, Rachmilewitz J, Galun E, Giladi H. TLR3 signaling in a hepatoma cell line is skewed towards apoptosis. *J Cell Biochem*. 2007;100(5):1301–1312.
19. Schmidt KN, Leung B, Kwong M, et al. APC-independent activation of NK cells by the Toll-like receptor 3 agonist double-stranded RNA. *J Immunol*. 2004;172(1):138–143.
20. Chew V, Chen J, Lee D, et al. Chemokine-driven lymphocyte infiltration: an early intratumoural event determining long-term survival in resectable hepatocellular carcinoma. *Gut*. 2012;61(3):427–438.
21. McCartney S, Vermi W, Gilfillan S, et al. Distinct and complementary functions of MDA5 and TLR3 in poly(I:C)-mediated activation of mouse NK cells. *J Exp Med*. 2009;206(13):2967–2976.
22. Chisari FV, Klopchin K, Moriyama T, et al. Molecular pathogenesis of hepatocellular carcinoma in hepatitis B virus transgenic mice. *Cell*. 1989;59(6):1145–1156.
23. Keng VW, Villanueva A, Chiang DY, et al. A conditional transposon-based insertional mutagenesis screen for genes associated with mouse hepatocellular carcinoma. *Nat Biotechnol*. 2009;27(3):264–274.
24. Hong M, Puaux AL, Huang C, et al. Chemotherapy induces intratumoral expression of chemokines in cutaneous melanoma, favoring T-cell infiltration and tumor control. *Cancer Res*. 2011;71(22):6997–7009.
25. Yu L, Chen S. Toll-like receptors expressed in tumor cells: targets for therapy. *Cancer Immunol Immunother*. 2008;57(9):1271–1278.
26. Sauder DN. The emerging role of immunotherapy in the treatment of non-melanoma skin cancers. *Nat Clin Pract Oncol*. 2005;2(7):326–327.
27. Murad YM, Clay TM. CpG oligodeoxynucleotides as TLR9 agonists: therapeutic applications in cancer. *BioDrugs*. 2009;23(6):361–375.
28. Salaun B, Zitvogel L, Asselin-Paturel C, et al. TLR3 as a biomarker for the therapeutic efficacy of double-stranded RNA in breast cancer. *Cancer Res*. 2011;71(5):1607–1614.
29. Hawkins MJ, Levin M, Borden EC. An Eastern Cooperative Oncology Group phase I-II pilot study of polyriboinosinic-polyribocytidylic acid poly-L-lysine complex in patients with metastatic malignant melanoma. *J Biol Response Mod*. 1985;4(6):664–668.
30. Yoneda K, Sugimoto K, Shiraki K, et al. Dual topology of functional Toll-like receptor 3 expression in human hepatocellular carcinoma: differential signaling mechanisms of TLR3-induced NF-kappaB activation and apoptosis. *Int J Oncol*. 2008;33(5):929–936.
31. Sivori S, Falco M, Carlomagno S, Romeo E, Moretta L, Moretta A. Heterogeneity of TLR3 mRNA transcripts and responsiveness to poly (I:C) in human NK cells derived from different donors. *Int Immunol*. 2007;19(12):1341–1348.
32. Lang KS, Georgiev P, Recher M, et al. Immunoprivileged status of the liver is controlled by Toll-like receptor 3 signaling. *J Clin Invest*. 2006;116(9):2456–2463.


## Funding


This research was funded by Singapore Immunology Network (SIgN) of the Biomedical Research Council, A*STAR, Singapore. This study was partly funded by a Hong Kong Research Grants Council Collaborative Research Grant (HKU 7/CRG/09 to IOLN). Mathias Heikenwalder was funded by a European Research Council starting grant.


## Notes


The funders did not have a role in the design of the study; the collection, analysis, and interpretation of the data; the writing of the manuscript; and the decision to submit the manuscript for publication. We wish to thank Dr Ksenija Slankamenac (University Hospital of Zurich, Zurich, Switzerland) for providing the patient samples and information; Dr Peter Schraml (University Hospital of Zurich, Zurich, Switzerland) for providing the patient formalin-fixed paraffin-embedded sections from the Zurich cohort; and Joyce Lee (University of Hong Kong, Hong Kong) for preparing the patient RNA and formalin-fixed paraffin-embedded samples from the Hong Kong cohort. We thank Dr Neil McCarthy (Insight Editing, London, UK) for manuscript editing. Our thanks are due to Dr Benjamin Toh, Dr Muly Tham, and Dr Lu-En Wai (Singapore Immunology Network, Singapore) for their help in harvesting mouse liver tumors and to Dr Michael Poidinger, Dr Bernett Lee, and Pavandip Singh Wasan (Singapore Immunology Network, Singapore) for help with the statistical analyses.

**Affiliations of authors:** Singapore Immunology Network (SIgN), Agency for Science, Technology and Research (A*STAR), Biopolis, Singapore (VC, CT, CH, AN, J-PA); Institute of Molecular and Cell Biology, Agency for Science, Technology and Research, Biopolis, Singapore (EB-C, NGC, NAJ); Department of Clinical Pathology, University Hospital of Zurich, Zurich, Switzerland (AW); Department of Pathology, Singapore General Hospital, Singapore (KHL); Department of Medical Oncology, National Cancer Centre, Singapore (HCT); Institute of Neuropathology, University Hospital Zurich, Zurich, Switzerland, and Institute of Virology, Technical University München/Helmholtz Zentrum München, Munich, Germany (MH); Department of Pathology and Queen Mary Hospital, State Key Laboratory for Liver Research, The University of Hong Kong, Hong Kong (IO-LN).